Disorder-induced rapid localization of electron-hole plasmas in highly excited $In_xGa_{1-x}N$ mixed crystals

Daisuke Hirano,[1] Takeshi Tayagaki,[1] and Yoshihiko Kanemitsu[1,2,*]

[1]*Institute for Chemical Research, Kyoto University, Uji, Kyoto 611-0011, Japan*
[2]*Photonics and Electronics Science and Engineering Center, Kyoto University, Kyoto 615-8510, Japan*

In mixed semiconductor crystals, random potential fluctuations cause localized band-tail states below the band edge and control the optical spectrum and dynamics. We report the influence of these band-tail states on the dynamics of electron-hole plasmas in highly excited $In_xGa_{1-x}N$ mixed crystals. Temporal changes in the luminescence spectrum of $In_xGa_{1-x}N$ mixed crystals and their band-gap renormalization are completely different from those of GaN crystals. Our findings show that holes are rapidly localized at band-tail states and that electron plasmas in the extended states determine the luminescence properties and band-gap renormalization of $In_xGa_{1-x}N$ mixed crystals.

As the primary material for optoelectronic applications in the blue and ultraviolet spectral regions,[1] the optical properties of GaN-based mixed crystals, such as $In_xGa_{1-x}N$ and $Al_xGa_{1-x}N$, have been extensively studied. In these mixed crystals, structural disorders induced by random fluctuations in the composition cause the formation of localized, so-called "band-tail," states below the mobility edge.[2] These band-tail states strongly affect the optical properties and exciton dynamics of mixed crystals.[3,4] Furthermore, due to the very small exciton Bohr radii in wide-gap $In_xGa_{1-x}N$ and $Al_xGa_{1-x}N$, these optical properties are very sensitive to spatial potential fluctuations. Between these properties and the ability to control their material properties by changing their compositional fraction x, wide-gap $In_xGa_{1-x}N$ and $Al_xGa_{1-x}N$ mixed crystals make excellent samples for studying the localization of excitons and electron-hole (e-h) plasmas in mixed crystals.

The existence of band-tail states drastically changes the exciton dynamics in semiconductors. Disorder-induced line broadening of optical transitions and localization of excitons and biexcitons are observed in semiconductor mixed crystals.[3–9] In addition, the localized states play an essential role in the excitonic optical gain and lasing processes in highly excited mixed crystals.[10,11] However, the effect of localized band-tail states on the formation and relaxation processes of e-h plasmas is not clear.[12,13] Moreover, two long-standing issues remain unresolved in the optical response of highly dense e-h plasmas: large discrepancies between the experimental observations and theoretical calculations of band-gap renormalization in wide-gap semiconductors[13,14] and the origin of excitonic photoluminescence (PL) and the transformation from e-h plasmas into Coulomb-bound pairs (excitons) in semiconductors.[15–18] Because free exciton PL is not observed in $In_xGa_{1-x}N$ mixed crystals even at elevated temperatures,[9] no spectral overlap occurs between e-h plasma and free exciton PL bands. Therefore, the time-resolved PL studies of $In_xGa_{1-x}N$ mixed crystals provide detailed information about e-h plasmas in highly excited semiconductors.

In this work, we examined the time-resolved PL spectrum of highly excited $In_xGa_{1-x}N$ mixed crystals at low tempera-

tures. The broad PL band, due to e-h plasmas, appears in the picosecond time scale. The rapid transformation from e-h plasmas to localized excitons occurs within several picoseconds. The band-gap shrinkage of the $In_xGa_{1-x}N$ mixed crystals is much smaller than that of GaN crystals. We conclude that holes are rapidly localized at band-tail states and that electron plasmas in the extended states determine the luminescence dynamics in $In_xGa_{1-x}N$ mixed crystals.

The 90-nm-thick $In_xGa_{1-x}N$ epitaxial layers were grown on a patterned sapphire substrate with a 5 μm GaN buffer layer.[19,20] The preparation and characterization of our samples were described in Ref. 20. Compositions of x =0.05 and 0.09 were chosen for investigation because defects in In-rich samples ($x>0.1$) strongly affect the luminescence dynamics, and the PL peak energy is too close to that of the GaN buffer layer in low In percentage samples (e.g., x=0.03). Epitaxial films were used for the study of the nature of e-h plasma dynamics in $In_xGa_{1-x}N$ mixed crystals because in the quantum well structures, the PL spectrum is strongly influenced by internal piezoelectric fields due to lattice constant mismatch.[21]

Wavelength-tunable femtosecond laser pulses were obtained from an optical parametric amplifier system based on a regenerative amplified Ti:sapphire laser. The pulse duration and the repetition rate were ~150 fs and 1 kHz, respectively. The typical laser spot size on the samples, as carefully measured using a knife-edge method, was 100 μm. For the time-resolved PL spectral measurements, an optical Kerr gate method was used in a 1-mm-thick quartz cell with toluene as the Kerr medium. Time resolution was 0.7 ps. The PL spectra were measured as a function of delay time using a liquid-nitrogen-cooled charge-coupled device with a 50 cm single monochromator.

PL spectra were measured under band-to-band excitation at 7 K. The excitation laser photon energy was set to E_x +175 ± 5 meV, where E_x is the lowest free exciton energy in each $In_xGa_{1-x}N$ sample: 3.496 eV for GaN, 3.292 eV for $In_xGa_{1-x}N$ (x=0.05), and 3.110 eV for $In_xGa_{1-x}N$ (x=0.09). This is because, under the same excitation intensity, the initial electron temperatures (or excess energies) are almost the same in all samples. The excitation laser intensities were
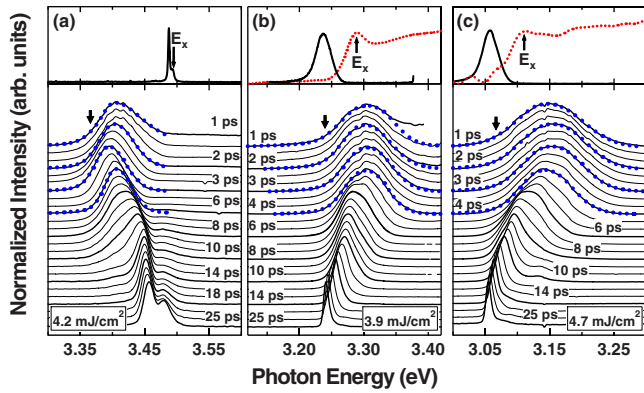
FIG. 1. (Color online) Time-resolved PL spectra of (a) GaN, (b) $In_xGa_{1-x}N$ ($x=0.05$), and (c) $In_xGa_{1-x}N$ ($x=0.09$) samples under extremely intense laser excitation at 7 K. Fits to the spectra are plotted by dots. The arrows at the 1 ps spectra indicate the renormalized band-gap energy ($\tilde{E}_g$) obtained from spectral fitting. The upper part shows time-integrated PL spectra under weak laser excitation (solid curves), the absorption spectra (dots), and the exciton free energy (E_x) for each sample.
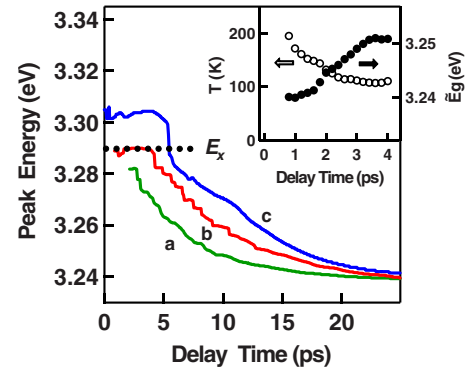

FIG. 2. (Color online) Temporal change of the PL peak energy in the $In_xGa_{1-x}N$ ($x=0.05$) mixed crystal sample for different excitation intensities: (a) 0.4 mJ/cm^2, (b) 1.0 mJ/cm^2, and (c) 3.9 mJ/cm^2. The inset shows the temporal change of the effective electron temperature and the renormalized band-gap energy at 3.9 mJ/cm^2.

varied between 0.4 and 4.5 mJ/cm^2. For comparison, time-resolved PL spectra were measured for 30-μm-thick GaN crystals under the same experimental conditions.

Figure 1 shows time-integrated and subpicosecond time-resolved PL spectra of (a) GaN, (b) $In_xGa_{1-x}N$ ($x=0.05$), and (c) $In_xGa_{1-x}N$ ($x=0.09$) samples. The time-integrated PL spectra were measured under weak laser excitation. The PL and optical absorption spectra are shown as solid and dotted curves, respectively, in the upper part of Figs. 1(a)–1(c). The lowest-exciton absorption peak is observed even in our $In_xGa_{1-x}N$ mixed crystal samples, and the arrows in the upper figures show the free exciton energy E_x. The Stokes shift between the E_x and PL peaks is 40–50 meV in the $In_xGa_{1-x}N$ mixed crystal samples; this large shift means the formation of localized band-tail states below the band edge.

The temporal change of the PL spectrum in GaN is different from that in $In_xGa_{1-x}N$. In the GaN crystal, under extremely intense excitation, the whole PL band appears at a lower energy, below E_x. A broad PL appears at early delay times up to about 10 ps. This broad band is due to the highly dense e-h plasmas. The blueshift of the PL peak energy occurs with an increase in delay time. The two clear peaks around 25 ps are due to the PL bands of the biexcitons (M line) and inelastic-exciton scattering (P line).

In contrast, in the $In_xGa_{1-x}N$ ($x=0.05$ and 0.09) mixed crystal, a broad PL appears at around E_x. This broad PL is clearly observed at delay times up to 5 ps. After an about 5 ps time delay, the PL peak energy is below the exciton energy E_x. At this lower energy, below E_x, the redshift of the PL peak energy occurs, and the PL spectral width becomes narrower and more symmetrical with increasing delay time. These large delay time behaviors can be explained by a localized exciton model with the electrons and holes relaxing into lower-energy localized states.[9]

The temporal change of the PL peak energy in the $In_xGa_{1-x}N$ ($x=0.05$) samples is plotted in Fig. 2 as a function

of delay time. At low excitation intensities, a broad PL band is not observed at the beginning, and the localized exciton PL is only seen in the low-energy region below E_x (see Fig. 2). The photoexcited carriers are rapidly localized at band-tail states.

Under high excitations above 1 mJ/cm^2, the PL peak energy appears above E_x at early delay times. When the PL peak energy reaches E_x (this time defined as τ_{local}), the temporal change of the PL spectrum abruptly occurs. At delay times shorter than τ_{local}, a broad PL band due to the e-h plasmas appears. At delay times longer than τ_{local}, the electrons and holes are localized into band-tail states. Similar behavior is observed in the $In_xGa_{1-x}N$ ($x=0.09$) sample. We found that the free exciton energy E_x is a good indicator for discriminating between e-h plasmas and excitons in mixed crystals. In addition, the band-gap energy in the e-h plasma region ($<\tau_{local}$) is much lower than E_x, and this behavior cannot be explained by piezoelectric effects, as will be discussed below.

To examine the dynamics of the highly dense e-h plasmas at early delay times, we calculated the spectral shape of spontaneous e-h plasma emission by a momentum conservation model with constant matrix elements[22] and by a nonmomentum conservation model.[23] In our case, the momentum conservation model reproduces well the experimental spectra, compared to the case of the nonmomentum conservation model. Hereafter, we discuss the e-h plasma dynamics using the momentum conservation model with a Lorentzian broadening of the Landsberg theory.[24,25] We applied the same approximated energy dependent Lorentzian width described in Ref. 24 for all samples. We followed this approach to determine the e-h pair density (n_p), the effective electron temperature (T_e) of the e-h pair, and the renormalized band-gap energy ($\tilde{E}_g$).

Effective electron and hole masses and dielectric constants for the $In_xGa_{1-x}N$ used in the e-h pair line shape analysis for concentrations of $x=0.05$ and 0.09 were determined using Vegard's rule with GaN and InN crystal parameters: For GaN, the hole mass was $m_h^*=1.66m_0$, the electron mass
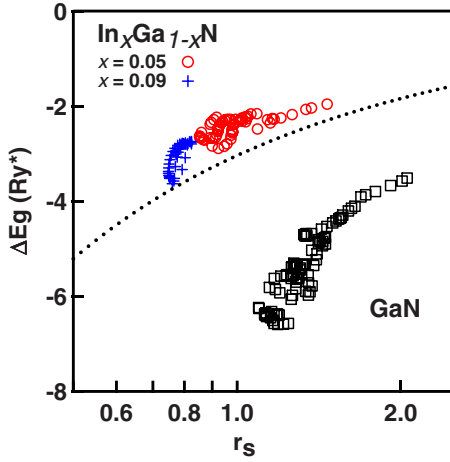
FIG. 3. (Color online) Universal plot of the band-gap renormalization and the normalized carrier density. The band-gap energy shrinkage ΔE_g is expressed in units of excitonic Rydberg energy Ry^* and the density in units of excitonic Bohr radius. The crosses, open circles, and squares represent the results for $In_{0.09}Ga_{0.91}N$, $In_{0.05}Ga_{0.95}N$, and GaN, respectively. The dotted line is a numerical calculation based on the Vashishta-Kalia theory.

$m_c^*=0.18m_0$, and the dielectric constant $\varepsilon=9.5$; for InN, the values were $m_h^*=1.63m_0$, $m_c^*=0.1m_0$, and $\varepsilon=15$,[26–28] where m_0 is the free electron mass. The calculated spectra are plotted with dots in Figs. 1(a)–1(c), and they fit the experimental spectra very well for early delay times. The spectrum widths of the e-h plasma luminescence in $In_xGa_{1-x}N$ and GaN are determined by the Fermi energy of the electrons, rather than that of the holes, because of the large mass mismatch.[29] As an example, the inset of Fig. 2 shows the temporal changes of $\tilde{E}_g$ and T_e evaluated from the spectral fitting of the $In_xGa_{1-x}N$ ($x=0.05$) sample at 3.9 mJ/cm². With an increase of delay time, the carrier density decreases. It is noted that the band-gap energy increases with delay time. This behavior is explained by many-body effects, rather than piezoelectric and thermal effects.

Just after laser excitation, the photoexcited electrons and holes in the extended states have enough kinetic energy to escape from the localized states. The effective electron temperature rapidly decreases and the lattice temperature increases through electron-phonon interactions. We estimated that the lattice temperature raise is less than 100 K and the thermal-induced redshift of the band-gap energy is negligibly small.[30] It is also experimentally confirmed that the band-gap renormalization is almost independent of electron temperature, but it is strongly dependent on e-h plasma density.[31] The plasma density, estimated from the PL line shape analysis, is kept to about 6.0×10^{18} cm⁻³ until the delay time reaches 5 ps, a value higher than the Mott transition density.

Figure 3 shows the universal plot of the band-gap shrinkage ΔE_g as a function of the parameter r_s in GaN and $In_xGa_{1-x}N$ mixed crystals. Here, ΔE_g is defined by the reduction of the band gap in units of exciton binding energy Ry^*,

$$\Delta E_g = (\tilde{E}_g - E_g)/Ry^*, \qquad (1)$$

and r_s is defined by the e-h density n_p and the exciton Bohr radius a_B,[13]

$$r_s = \left(\frac{4\pi a_B^3 n_p}{3}\right)^{-1/3}. \qquad (2)$$

We consider that in high-density e-h plasma regime, the piezoelectric field effect on the PL spectra is negligibly small because of e-h plasma screening effects. The band-gap energies of unstrained $In_xGa_{1-x}N$ crystals, $E_g(x)$, are needed for the evaluation of ΔE_g. Unfortunately, their values are unclear experimentally because of the piezoelectric effects. Then, we estimated $E_g(x)$ using the following approximation:

$$E_g(x) = xE_g(\text{InN}) + (1-x)E_g(\text{GaN}) - x(1-x)b, \qquad (3)$$

where $E_g(\text{InN})$ and $E_g(\text{GaN})$ are the band-gap energies of InN (0.78 eV) and GaN (3.51 eV), respectively, and b is the bowing constant in the virtual crystal approximation model.[32] Several values of the bowing parameters have been discussed for the band-gap energy estimation of $In_xGa_{1-x}N$ mixed crystals.[28] We use the bowing constant of 1.4 eV according to Ref. 28. The calculated band-gap energy is also consistent with the experimentally estimated exciton energy E_x in our InGaN samples. Broad e-h plasma PL is clearly observed at excitation intensities above 1.0 mJ/cm². Data obtained at varying excitation intensities above 1.0 mJ/cm² are summarized in this figure. Figure 3 clearly shows that the r_s dependence of the band-gap shrinkage in $In_xGa_{1-x}N$ mixed crystals is completely different from that of GaN; it is much smaller, even though the material parameters of GaN and $In_xGa_{1-x}N$ are very similar to each other.

In highly excited semiconductors, the band-gap shrinkage is caused by the many-body effects in highly dense e-h systems. The magnitude of the band-gap shrinkage in narrow-gap semiconductors, such as Si, Ge, and GaAs, is well explained by the universal formula of the Vashishta–Kalia (VK) model.[33] The dotted line in the figure is given by the VK theory with the e-h exchange interaction neglected. However, in GaN crystals, a large discrepancy exists between the experimental observations and the theoretical VK calculation, as seen in Fig. 3. In wide-gap semiconductors possessing large exciton binding energies, such as GaN, the e-h exchange and excitonic effects, in addition to the electron-electron (e-e) and hole-hole (h-h) interactions, play an essential role in the band-gap renormalization.[14] Therefore, it is believed that the reduction of the e-h interactions is the principal cause of the differences between GaN and $In_xGa_{1-x}N$ crystals.

As noted above, the hole masses in $In_xGa_{1-x}N$ mixed crystals are an order of magnitude greater than the electron masses. This large mass mismatch plays an essential role in the relaxation of e-h plasmas. The energy loss rate of holes by phonons is much faster than that of electrons.[34] The holes are rapidly relaxed to the top of the valence band and localized into the band-tail states. We believe that this rapid hole localization plays an essential role in the band-gap renormalization reduction. Many-body interactions between holes and electrons are related to their wave function overlap.[29,35] In our case, where electrons exist at delocalized extended states above the band edge and holes at localized band-tail states below the band edge, the many-body interactions between them are very weak. In $In_xGa_{1-x}N$ mixed crystals, the reduc-

tion of the e-h interactions is caused by rapid hole localization, and the electron plasmas determine their PL dynamics and spectrum.

In conclusion, we have shown the importance of e-h plasma localization on the PL dynamics of $In_xGa_{1-x}N$ mixed crystals leading to a smaller band-gap renormalization in $In_xGa_{1-x}N$ mixed crystals compared to GaN crystals. Our findings indicate that holes are rapidly localized at band-tail states and that electron plasmas in the extended states determine the PL dynamics. Our experimental approach of using

mixed crystals strongly suggests a method for solving the long-standing problems of very large band-gap renormalization in wide-gap semiconductors and the transformation from e-h plasma to excitons in highly excited semiconductors.

*Corresponding author. kanemitu@scl.kyoto-u.ac.jp

[1] S. Nakamura, S. Pearton, and G. Fasol, *The Blue Laser Diode* (Springer, Berlin, 2000).

[2] See, for example, N. F. Mott and E. A. Davis, *Electronic Processes in Non-Crystalline Materials* (Oxford University Press, Oxford, 1979).

[3] E. Cohen and M. D. Sturge, Phys. Rev. B **25**, 3828 (1982).

[4] S. Permogorov, A. Rentitskii, S. Verbin, G. O. Müller, P. Flögel, and M. Nikiforova, Phys. Status Solidi B **113**, 589 (1982).

[5] G. Noll, U. Siegner, S. G. Shevel, and E. O. Göbel, Phys. Rev. Lett. **64**, 792 (1990).

[6] J. Y. Bigot, A. Daunois, J. Oberle, and J. C. Merle, Phys. Rev. Lett. **71**, 1820 (1993).

[7] W. Langbein and J. M. Hvam, Phys. Rev. B **59**, 15405 (1999).

[8] Y. Yamada, Y. Ueki, K. Nakamura, T. Taguchi, A. Ishibashi, Y. Kawaguchi, and T. Yokogawa, Phys. Rev. B **70**, 195210 (2004).

[9] Y. Kanemitsu, K. Tomita, and H. Inouye, Appl. Phys. Lett. **87**, 151120 (2005); Y. Kanemitsu, K. Tomita, D. Hirano, and H. Inouye, *ibid.* **88**, 121113 (2006).

[10] J. Ding, H. Jeon, T. Ishihara, M. Hagerott, A. V. Nurmikko, H. Luo, N. Samarth, and J. Furdyna, Phys. Rev. Lett. **69**, 1707 (1992).

[11] A. Satake, Y. Masumoto, T. Miyajima, T. Asatsuma, and M. Ikeda, Phys. Rev. B **60**, 16660 (1999).

[12] F. A. Majumder, S. Shevel, V. G. Lyssenko, H. E. Swoboda, and C. Klingshirn, Z. Phys. B: Condens. Matter **66**, 409 (1987).

[13] C. Klingshirn, *Semiconductor Optics*, 3rd ed. (Springer, Berlin, 2006).

[14] T. J. Inagaki and M. Aihara, Phys. Rev. B **65**, 205204 (2002).

[15] L. Kappei, J. Szczytko, F. Morier-Genoud, and B. Deveaud, Phys. Rev. Lett. **94**, 147403 (2005).

[16] R. A. Kaindl, M. A. Carnahan, D. Hägele, R. Lövenich, and D. S. Chemla, Nature (London) **423**, 734 (2003).

[17] S. W. Koch, M. Kira, G. Khitrova, and H. M. Gibbs, Nat. Mater. **5**, 523 (2006).

[18] F. Binet, J. Y. Duboz, J. Off, and F. Scholz, Phys. Rev. B **60**, 4715 (1999).

[19] K. Tadatomo, H. Okagawa, Y. Ohuchi, T. Tsunekawa, Y. Imada,

M. Kato, and T. Taguchi, Jpn. J. Appl. Phys., Part 2 **40**, L583 (2001).

[20] C. Sasaki, H. Naito, M. Iwata, H. Kudo, Y. Yamada, T. Taguchi, T. Jyouichi, H. Okagawa, K. Tadatomo, and H. Tanaka, J. Appl. Phys. **93**, 1642 (2003).

[21] E. Kuokstis, J. W. Yang, G. Simin, and M. Asif Khanb, R. Gaska, and M. S. Shur, Appl. Phys. Lett. **80**, 977 (2002).

[22] R. Cingolani, H. Lage, L. Tapfer, H. Kalt, D. Heitmann, and K. Ploog, Phys. Rev. Lett. **67**, 891 (1991).

[23] E. Göbel, Appl. Phys. Lett. **24**, 492 (1974).

[24] R. Martin and H. Störmer, Solid State Commun. **22**, 523 (1977).

[25] P. Landsberg, Phys. Status Solidi **15**, 623 (1966).

[26] Y. C. Yeo, T. C. Chong, and M. F. Li, J. Appl. Phys. **83**, 1429 (1998).

[27] M. Suzuki, T. Uenoyama, and A. Yanase, Phys. Rev. B **52**, 8132 (1995).

[28] I. Vurgaftman and R. Mayer, J. Appl. Phys. **94**, 3675 (2003).

[29] V. D. Kulakovskii, E. Lach, A. Forchel, and D. Grutzmacher, Phys. Rev. B **40**, 8087 (1989).

[30] Using a value of the heat capacity reported in W. Shan, T. J. Schmidt, X. H. Yang, S. J. Hwang, and J. J. Song, Appl. Phys. Lett. **66**, 985 (1995), the lattice temperature raise caused by all excess energy of excited carriers is estimated to be less than 100 K. This calculation and the inset of Fig. 2 imply that the lattice temperature is less than about 100 K during several picoseconds. The redshift of band-gap energy from 7 to 100 K is much smaller than the values of ΔE_g.

[31] In order to clarify the effect of the initial electron temperature on e-h plasma dynamics, PL spectra of GaN were measured under the band-to-band and exciton-resonant excitations. We found that there is no significant difference in ΔE_g between two different excitations.

[32] M. Cardona, Phys. Rev. **129**, 69 (1963).

[33] P. Vashishta and R. K. Kalia, Phys. Rev. B **25**, 6492 (1982).

[34] R. Ulbrich, Phys. Rev. B **8**, 5719 (1973).

[35] C. Weber, C. Klingshirn, D. S. Chemla, D. A. B. Miller, J. E. Cunningham, and C. Ell, Phys. Rev. B **38**, 12748 (1988).